

Stability for Shape Comparison Model*

Wei Zhu[†] and Tony Chan[‡]

March 4, 2003

Abstract

In this paper, we would like to give a proof of the stability for shape comparison model, proposed by Paragios, Rousson and Ramesh[3], which states that once an object is perturbed a little, the shape difference between the two objects (the original one and the perturbed one) defined by the model is also small, and vice versa.

1. Introduction

Shape is an important issue in image processing. The shape of an object in an image is uniquely determined by its boundary, or in briefly, can be characterized by its boundary. Given the boundary of an object or a closed curve in R^2 , there exists uniquely a level set function, which is proposed by Osher and Sethian [2], i.e, a signed distance function with inside positive and outside negative related to the boundary. Thus shapes can be characterized by the corresponding signed distance functions, which is proposed by Paragios, Rousson and Ramesh [3].

Explicitly, for any object Ω in an image R , its shape only depends on its boundary $\partial\Omega$. Then there exists a unique signed distance function related to this boundary, i.e, a viscosity solution can be found to the following equation:

$$|\nabla\varphi|=1 \tag{1}$$

$$\varphi|_{\partial\Omega}=0 \tag{2}$$

with $\varphi(x) < 0$ as $x \in R \setminus \Omega$, $\varphi(x) > 0$ as $x \in \Omega \setminus \partial\Omega$. Here, we assume Ω as a closed set.

Shape is invariant to translation, dilation and rotation. For example, given an ellipse as its boundary, if one translates, dilates and rotates it to be another

*This work has been supported partly by ONR contract N00014-96-1-0277, NSF contract DMS-9973341 and NIH contract P20 MH65166.

[†]Department of Mathematics, University of California, Los Angeles, 405 Hilgard Avenue, Los Angeles, CA 90095-1555. E-mail: wzhu@math.ucla.edu

[‡]Department of Mathematics, University of California, Los Angeles, 405 Hilgard Avenue, Los Angeles, CA 90095-1555. E-mail: TonyC@college.ucla.edu

object, the new one must also be an ellipse. Inversely, if two objects have the same shapes, one object can be converted by translation, dilation and rotation to the other object. This means, instead of seeing a shape as an isolated one, a shape can be defined as an equivalent relation of objects, that is to say, for any two objects with the same shape, they belong to the same equivalent class. Different objects with same shapes have different signed distance functions, however, they can be converted to each other by a suitable transformation. For instance, if Ω_2 has the same shape of Ω_1 , and let φ_1 be the signed distance function to Ω_1 , then the signed distance function φ_2 to Ω_2 satisfies:

$$\varphi_2(x_1, x_2) = r\varphi_1 \left[\frac{(x_1 - a) \cos \theta + (x_2 - b) \sin \theta}{r}, \frac{-(x_1 - a) \sin \theta + (x_2 - b) \cos \theta}{r} \right] \quad (3)$$

for a group of suitable parameters a, b, θ, r , where (a, b) means the center for rotation, θ the angle of rotation, r the scaling factor. This expression could be reached as the composition of three functions developed by translation, dilation and rotation. For example, if an object Ω is translated by a vector (a, b) , then the signed distance function $\phi(x, y) = \varphi(x - a, y - b)$, where φ is the signed distance function according to Ω .

In this way, we denote the above equivalent class of Ω_1 as $\Gamma(\Omega_1)$, or without confusion, we also denote it as $\Gamma(\varphi_1)$ with φ_1 as the corresponding signed distance function to Ω_1 , i.e. $\Gamma(\Omega_1)$ is identified as $\Gamma(\varphi_1) = \{\varphi_2 : a, b, r, \theta \in R^1\}$, where φ_2 is expressed in (3).

With these notations, as discussed in Paragios, Rousson and Ramesh's paper [3], the shapes comparison model can be given as follows: Given two objects, Ω_1, Ω_2 , and the corresponding signed distance functions φ_1, φ_2 , respectively. we define an *Index* function as,

$$Index(\varphi_1, \varphi_2) = \min_{\tilde{\varphi} \in \Gamma(\varphi_2)} \int_{\Omega} (\varphi_1 - \tilde{\varphi})^2 dx \quad (4)$$

where the minimum is obtained as $\tilde{\varphi}$ runs over all signed distance functions in $\Gamma(\varphi_2)$. We may also use $Index(\Omega_1, \Omega_2)$ to denote $Index(\varphi_1, \varphi_2)$.

From the definition of this *Index* function, it is easy to see: if Ω_1 and Ω_2 belong to the same equivalent class, then $Index(\Omega_1, \Omega_2) = 0$. Moreover, $Index(\varphi_1, \varphi_2)$ is not symmetric about φ_1 and φ_2 .

To apply the above index function, several questions will arise. One of the questions is: can this function describe the perturbation of an object (shape)? In another word, if there is a small perturbation for an object Ω_1 , denote the object as Ω_{1per} , will the $Index(\Omega_1, \Omega_{1per})$ become far from zero? And, if given two objects Ω_1, Ω_2 , if $Index(\Omega_1, \Omega_2)$ is close to zero, can we claim that there is only a small perturbation between the shapes of Ω_1 and Ω_2 ? Moreover, if given three objects $\Omega_1, \Omega_2, \Omega_3$, and suppose $Index(\Omega_1, \Omega_2) < Index(\Omega_1, \Omega_3)$, can we reach the conclusion that the shape of Ω_1 is more similar to that of Ω_2 than to Ω_3 ?

In section 2, we would like to provide the proof for the positive answers of these questions, for which we call the stability of the shape comparison model, and in section 3 we present experimental results to validate the statements. A conclusion is followed in section 4.

2. Stability for shape comparison model

Before proving the theorem about the stability for the shape comparison model, we would like to provide the existence for the minimizer of the *index* function.

Theorem 1. *Given two objects Ω_1, Ω_2 in an image R , and the corresponding signed distance functions φ_1, φ_2 respectively, there exists an object $\hat{\Omega} \in \Gamma(\Omega_2)$, and signed distance function $\hat{\varphi}$, such that*

$$\int_R (\varphi_1(x) - \hat{\varphi}(x))^2 dx = \text{Index}(\Omega_1, \Omega_2) = \min_{\varphi \in \Gamma(\varphi_2)} \int_R (\varphi_1(x) - \varphi(x))^2 dx.$$

Proof. Denote $\mu = \text{Index}(\Omega_1, \Omega_2)$. By the definition, there is a sequence of shapes $\hat{\Omega}_n$, and signed distance functions $\hat{\varphi}_n$, such that $\int_R (\varphi_1(x) - \hat{\varphi}_n(x))^2 dx \rightarrow \mu$, as $n \rightarrow \infty$.

Notice that for any $\phi \in \Gamma(\Omega_2)$, there uniquely exist a four-tuple (θ, r, a, b) , where $\theta \in [0, 2\pi]$ means the rotation angle, $r > 0$ the scaling factor, $(a, b) \in \mathbb{R}^2$ the center, such that

$$\phi(x_1, x_2) = r\varphi_2 \left[\frac{(x_1 - a) \cos \theta + (x_2 - b) \sin \theta}{r}, \frac{-(x_1 - a) \sin \theta + (x_2 - b) \cos \theta}{r} \right].$$

So, for the sequence $\hat{\varphi}_n$, there exist a sequence of four-tuple $(\theta_n, r_n, a_n, b_n)$, $n = 1, 2, 3, \dots$. As the induced sequence θ_n, r_n, a_n, b_n are bounded, we can choose a subsequence of index $\{n_k\}_{k=1}^{\infty}$, such that $\theta_{n_k}, r_{n_k}, a_{n_k}, b_{n_k}$ are all convergent subsequences. Denote by θ_0, r_0, a_0, b_0 as the limit for the convergent subsequences, respectively. Then we obtain a function $\hat{\varphi}$ defined as,

$$\hat{\varphi}(x_1, x_2) = r_0\varphi_2 \left[\frac{(x_1 - a_0) \cos \theta_0 + (x_2 - b_0) \sin \theta_0}{r_0}, \frac{-(x_1 - a_0) \sin \theta_0 + (x_2 - b_0) \cos \theta_0}{r_0} \right],$$

$\hat{\varphi} \in \Gamma(\Omega_2)$ and $\int_R (\varphi_1(x) - \hat{\varphi}(x))^2 dx = \mu$. ♠

Remark. Apparently, we can only get existence, no uniqueness for $\hat{\Omega}$. For instance, let Ω_1 be a unit disk, and Ω_2 be any shape. Suppose $\hat{\Omega}$ be the shape determined by the above theorem, then if we rotate it about the center of Ω_1 , the result objects are all the minimizers.

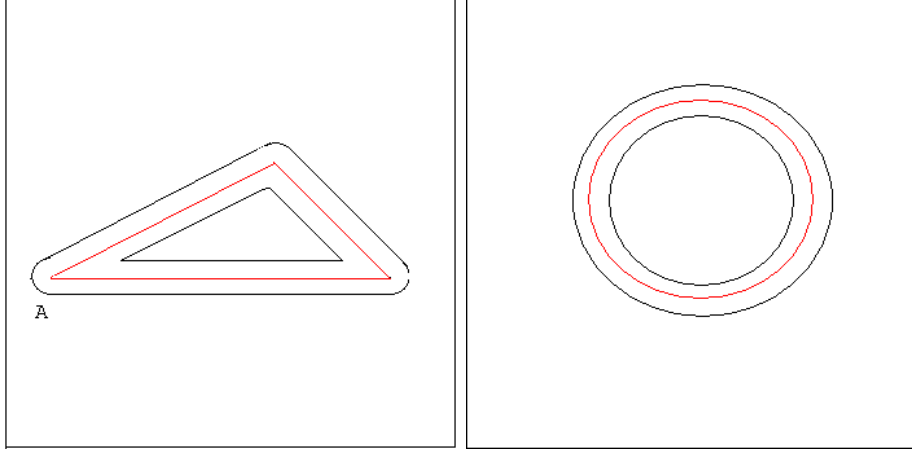


Figure 1. In the left graph, the red curve represents a triangle Ω^1 , with point A being a vertex, and $\Omega_{1+r_1}^1, \Omega_{1-r_2}^1$ are denoted by the two black curves. And the three curves in the right graph represent a disk Ω^2 , $\Omega_{1+r_1}^2, \Omega_{1-r_2}^2$ respectively. It can be seen that $d(A, \partial\Omega_{1-r_2}^1) > d(x, \partial\Omega_{1-r_2}^2) = r_2$, for any $x \in \partial\Omega^2$. This demonstrates that only introducing r_1 and r_2 is insufficient, which leads to the Definition 2.

To prove the theorem about the stability, it is necessary to explore the concept of *Perturbation* of an object.

Let R be a rectangle region, Ω be an object inside R , and φ be the corresponding signed distance function.

Denote

$$\Omega_{1+r_1} = \{x \in R : \text{distance}(x, \Omega) \leq r_1, r_1 \geq 0\}$$

and

$$\Omega_{1-r_2} = \{x \in \Omega : \text{distance}(x, \partial\Omega) \geq r_2, r_2 \geq 0\},$$

where the *distance* is the ordinary Euclidean distance in R^2 . In the following, we will use $d(\cdot, \cdot)$ to represent $\text{distance}(\cdot, \cdot)$.

Definition 1: we say $\tilde{\Omega}$ is a *perturbation* of an object Ω , if there exist two nonnegative numbers r_1 and r_2 such that $\Omega_{1-r_2} \subseteq \tilde{\Omega} \subseteq \Omega_{1+r_1}$.

However, as Ω could be very complicated, only the two numbers r_1 and r_2 are not enough to describe the perturbation, which is illustrated by Figure 1.

In Figure 1, a triangle Ω^1 and a disk Ω^2 are shown on the left and right graphs respectively. With the same perturbation parameters r_1 and r_2 for both

Ω^1 and Ω^2 , $d(A, \partial\Omega_{1-r_2}^1)$ is larger than $d(x, \partial\Omega_{1-r_2}^2)$ for any x on $\partial\Omega^2$. As the angle at the vertex A becomes smaller, $d(A, \partial\Omega_{1-r_2}^1)$ will be larger. This situation does not happen to the disk. This means, additional parameters should be introduced to describe the perturbation according to the shape itself.

Definition 2: Let Ω_{1+r_1} and Ω_{1-r_2} defined as in definition 1, we introduce two parameters s_1 and s_2 according to the region Ω as: $s_1 = \max_{x \in \partial\Omega} d(x, \partial\Omega_{1+r_1})$, $s_2 = \max_{x \in \partial\Omega} d(x, \partial\Omega_{1-r_2})$.

By the definition, it can be seen that $r_1 \leq s_1$ and $r_2 \leq s_2$. In the two cases shown in Figure 1, for the triangle, $s_1 = r_1$, $s_2 =$ the largest one of the three distances from the vertices to $\partial\Omega_{1-r_2}^{tri}$, while for the disk, $s_1 = r_1$ and $s_2 = r_2$.

Moreover, by the definition 2, for the triangle in Figure 1, as the angle at vertex A becomes small, s_2 will become large, which is mentioned above. In fact, it is easy to see that $s_2 = \frac{r_2}{\sin(\angle A/2)}$, where $\angle A$ denotes the angle at vertex A . This simple fact leads the following lemma.

Lemma 1. For a given object $\Omega \subseteq R^2$, and Ω_{1+r_1} , Ω_{1-r_2} defined as before, then there exists two positive constants C_Ω^1 and C_Ω^2 which depend on Ω , such that $s_i \leq C_\Omega^i r_i$, $i = 1, 2$.

Theorem 2. Let R be an image, Ω be an object in this image, $\tilde{\Omega}$ be any small perturbation of Ω , with $\Omega_{1-r_2} \subseteq \tilde{\Omega} \subseteq \Omega_{1+r_1}$, where

$$r_1 = \inf \left\{ r > 0 : \tilde{\Omega} \subseteq \Omega_{1+r} \right\}$$

and

$$r_2 = \inf \left\{ r > 0 : \Omega_{1-r} \subseteq \tilde{\Omega} \right\},$$

and s_1, s_2 are defined as in Definition 2 according to Ω_{1+r_1} and Ω_{1-r_2} . And let φ and $\tilde{\varphi}$ be the corresponding signed distance functions to $\Omega, \tilde{\Omega}$ respectively.

Then, there exist two positive constants C_1 and C_2 , which are independent of r_1 and r_2 , such that

$$C_2 r^4 \leq \int_R (\varphi(x) - \tilde{\varphi}(x))^2 dx \leq C_1 r^2$$

where $r = \max(r_1, r_2)$, which can be called as the scale of perturbation of $\tilde{\Omega}$ with respect to Ω .

Proof. First, we want to prove the left side of the inequalities. A graph of the boundaries of Ω_{1+r_1} , Ω , Ω_{1-r_2} and $\tilde{\Omega}$ are shown in Figure 2. Without loss of generality, we assume $r_1 \geq r_2$. Then there exists a point $a \in \partial\tilde{\Omega}$, such

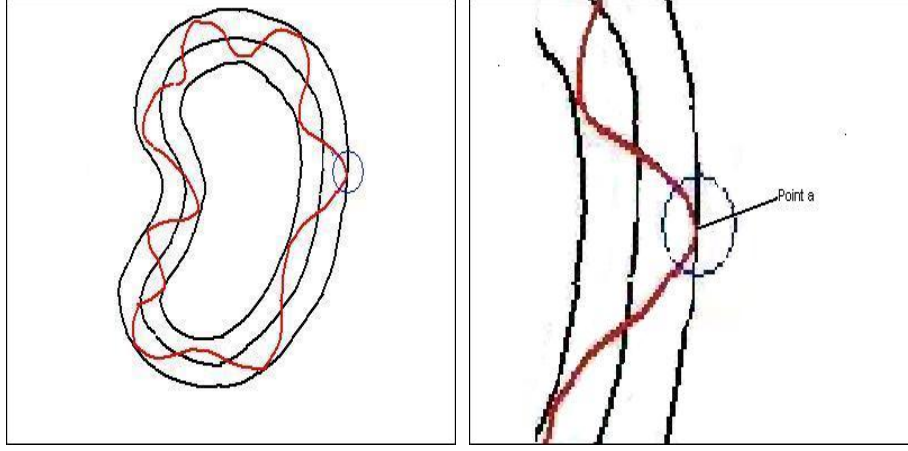


Figure 2. An object and a perturbed one. For the graph on the left, the three black curves represent the boundaries of Ω_{1+r_1} , Ω , Ω_{1-r_2} respectively from outside to inside, While red curve denotes that of the perturbed shape $\tilde{\Omega}$. A circle $B(a, r_1/4)$ is also shown on the graph. The graph on the right is a large scale version of the circle.

that $d(a, \Omega) = r_1$. Choose a disk centered at a with the radius $r_1/4$, denoted by $B(a, r_1/4)$. Next, we consider this small ball, which is divided by the boundary of $\partial\tilde{\Omega}$ into two parts denoted by B_{right} and B_{left} as shown in a large scale in the graph on the right of Figure 2, where the red curve is the boundary of $\partial\tilde{\Omega}$. That is, $B(a, r_1/4) = B_{left} \cup B_{right}$, where $B_{left} = \{x \in B(a, r_1/4) : \tilde{\varphi}(x) \geq 0\}$, $B_{right} = \{x \in B(a, r_1/4) : \tilde{\varphi}(x) \leq 0\}$.

Then for any point $x \in B_{right}$, $d(x, \partial\tilde{\Omega}) \leq d(x, a) \leq r_1/4$, and since $\partial\Omega$ is compact, there exists a point $p \in \partial\Omega$, such that $d(x, \partial\Omega) = d(x, p)$, and as $d(x, p) > d(a, p) - d(a, x)$, $d(a, p) \geq d(a, \partial\Omega)$, we get $d(x, \partial\Omega) = d(x, p) > d(a, \partial\Omega) - d(a, x) > r_1 - r_1/4 = 3r_1/4$. Therefore, by the definition of signed distance function, for any point $x \in B_{right}$, $\varphi(x) < -3r_1/4$, $\tilde{\varphi}(x) \geq -r_1/4$, since $x \notin \Omega$ and $x \notin \tilde{\Omega}$. So, $|\varphi(x) - \tilde{\varphi}(x)| \geq 3r_1/4 - r_1/4 = r_1/2$.

Similarly, for any point $x \in B_{left}$, $d(x, \partial\Omega) > d(a, \partial\Omega) - d(a, x) \geq r_1 - r_1/4 = 3r_1/4$. Then $\varphi(x) \leq -3r_1/4$ and clearly $\tilde{\varphi}(x) \geq 0$, as $x \in \tilde{\Omega}$ and $x \notin \Omega$. Also, $|\varphi(x) - \tilde{\varphi}(x)| \geq 3r_1/4 > r_1/2$.

In summary, for any $x \in B(a, r_1/4)$, $|\varphi(x) - \tilde{\varphi}(x)| \geq r_1/2$. we have

$$\begin{aligned} & \int_R (\varphi(x) - \tilde{\varphi}(x))^2 dx \\ & \geq \int_{B(a, r_1/4)} (\varphi(x) - \tilde{\varphi}(x))^2 dx > \left(\frac{r_1}{2}\right)^2 |B(a, r_1/4)| = \frac{\pi}{64} r_1^4 = C_2 r_1^4, \end{aligned}$$

where $|\cdot|$ means the area. Thus, the left side inequality is obtained.

Second, we prove the right side. As shown in the Figure 2, the rectangle R is divided into three subregions, that is, $R \setminus \Omega_{1+r_1}$, Ω_{1-r_2} and $\Omega_{1+r_1} \setminus \Omega_{1-r_2}$. We will estimate the difference $|\varphi(x) - \tilde{\varphi}(x)|$ as x belongs to each of the three subregions.

If $x \in R \setminus \Omega_{1+r_1}$, we want to show $|d(x, \Omega) - d(x, \tilde{\Omega})| \leq \max(s_1, s_2)$. In fact, it is easy to see that $d(x, \Omega_{1+r_1}) \leq d(x, \Omega) \leq d(x, \Omega_{1-r_2})$, and $d(x, \Omega_{1+r_1}) \leq d(x, \tilde{\Omega}) \leq d(x, \Omega_{1-r_2})$. Then $|d(x, \Omega) - d(x, \tilde{\Omega})| \leq \max(d(x, \Omega) - d(x, \Omega_{1+r_1}), d(x, \Omega_{1-r_2}) - d(x, \Omega))$. For $d(x, \Omega_{1-r_2}) - d(x, \Omega)$, since there exists a point $p \in \partial\Omega$, such that $d(x, p) = d(x, \partial\Omega)$, and there exists a point $q \in \partial\Omega_{1-r_2}$, such that $d(p, q) \leq s_2$, therefore, $d(x, \Omega_{1-r_2}) \leq d(x, q) < d(x, p) + d(p, q) \leq d(x, \partial\Omega) + s_2$, that is, $d(x, \Omega_{1-r_2}) - d(x, \Omega) \leq s_2$. Similarly, $d(x, \Omega) - d(x, \Omega_{1+r_1}) \leq s_1$. So, $|d(x, \Omega) - d(x, \tilde{\Omega})| \leq \max(s_1, s_2)$. Then by the definition of signed distance function, $|\varphi(x) - \tilde{\varphi}(x)| \leq \max(s_1, s_2)$.

Similarly, we have as $x \in \Omega_{1-r_2}$ or $\Omega_{1+r_1} \setminus \Omega_{1-r_2}$, $|\varphi(x) - \tilde{\varphi}(x)| \leq \max(s_1, s_2)$.

By lemma 1, $s_i \leq C_{\Omega}^i r_i$, $i = 1, 2$, hence $|\varphi(x) - \tilde{\varphi}(x)| \leq \max(s_1, s_2) \leq \max(C_{\Omega}^1 r_1, C_{\Omega}^2 r_2) \leq Cr$, where $C = \max(C_{\Omega}^1, C_{\Omega}^2)$.

In summary, for any $x \in R$, $|\varphi(x) - \tilde{\varphi}(x)| \leq Cr$. Therefore, we obtain the following,

$$\int_R (\varphi(x) - \tilde{\varphi}(x))^2 dx \leq |R| (Cr)^2 = |R| C^2 r^2 = C_1 r^2. \quad \spadesuit$$

Remark. This theorem states that when a perturbation is exerted on an object, the variance between the signed distance functions could be dominated by *the scale of perturbation* between the two objects, and which inversely can be determined by the variance. It seems that it is far away from what we want to get, since we just estimate for $\int_R (\varphi(x) - \tilde{\varphi}(x))^2 dx$, not $Index(\varphi, \tilde{\varphi})$. However, it provides an important clue to get the stability for shape comparison model and define the similarity between the shapes of any two objects.

In fact, given any two objects Ω_1 and Ω_2 , by theorem 1, there exists an object $\hat{\Omega} \in \Gamma(\Omega_2)$, and a signed distance function $\hat{\varphi} \in \Gamma(\varphi_2)$, such that $\int_R (\varphi_1(x) - \hat{\varphi}(x))^2 dx = Index(\Omega_1, \Omega_2)$. Then we can apply Theorem 2 for objects Ω_1 and $\hat{\Omega}$ to get the inequalities, which provides us the connection between $Index(\Omega_1, \Omega_2)$ and *the scale of perturbation* r of $\hat{\Omega}$ with respect to Ω_1 . As *the scale of perturbation* r exists uniquely, we may also call it as *the scale of perturbation* of Ω_2 with respect to Ω_1 .

Moreover, *the scale of perturbation* r can also be employed to describe the similarity between any two shapes of objects. It can be seen that $r = 0$ means the two shapes are the same, and the larger the r , the less similar the two shapes. In the next section, we will show some experiments that an equilateral polygon looks more like a disk as the number of the gon increases, which is reasonable.

In summary, we have the following theorem.

Theorem 3. *Given any two objects Ω_1 and Ω_2 , let $\mu = Index(\Omega_1, \Omega_2)$, and r be the scale of perturbation of Ω_2 with respect to Ω_1 , then r is dominated by μ , and μ also determines r .*

Proof. By theorem 1, there exists an object $\widehat{\Omega} \in \Gamma(\Omega_2)$, and signed distance function $\widehat{\varphi}$, such that $\int_R (\varphi_1(x) - \widehat{\varphi}(x))^2 dx = Index(\Omega_1, \Omega_2)$. Applying theorem 2 to Ω_1 and $\widehat{\Omega}$, we can get *the scale of perturbation* r of $\widehat{\Omega}$ with respect to Ω_1 , satisfying: $C_2 r^4 \leq \int_R (\varphi(x) - \widehat{\varphi}(x))^2 dx \leq C_1 r^2$, that is $C_2 r^4 \leq \mu \leq C_1 r^2$, where C_1 and C_2 are independent of r . ♠

Remark. By this theorem, we may answer the questions given at the end of the introduction. First, if Ω_2 is a small perturbation of Ω_1 , then $Index(\Omega_1, \Omega_2)$ will be close to zero, and as $Index(\Omega_1, \Omega_2)$ is close to zero, *the scale of perturbation* of Ω_2 with respect to Ω_1 should also close to zero, which states that the shapes of Ω_1 and Ω_2 are similar. Second, if *the scale of perturbation* of Ω_2 with respect to Ω_1 is less than that of Ω_3 with respect to Ω_1 , we can see the shape of Ω_2 is more close to the shape of Ω_1 than Ω_3 to Ω_1 .

3. Experiments

In this section, we provide some experiments of shape comparison to validate our statements. The three values of r_1, r_2 and $Index$ will be given for each experiments, and a relation between $r = \max(r_1, r_2)$ and $Index$ for almost similar shapes will be shown as well.

In the following graphs, the black one represents an object, while the white curve represents another object in the way that the white curve is the boundary of the object.

The first two experiments show the process of shape comparisons of two equilateral triangles (Figure 3.1) and two equilateral pentagons (Figure 3.2). We may see the two objects overlap, that is, $r = 0$, and $Index = 0$, which validates the inequalities in Theorem 2.

The third example shows the comparison results between a disk and three equilateral polygons, that is, equilateral triangle, square and pentagon (Figure 3.3). From the listed values, it can be seen that as the number of gons increases, the value of $Index$ and *the scale of perturbation* r will both decrease. This coincides with human visual.

The fourth example shows the comparison results between an equilateral triangle and some similar shapes (Figure 3.4), and a table (Table 1) is provided to demonstrate the relation between $Index$ and *the scale of perturbation* r .

4. Conclusion

In this paper, by introducing *the scale of perturbation*, we give the proof of the stability for the shape comparison model proposed by Paragios, Rousson and Ramesh[3], which states that once an object is perturbed a little, the shape difference between the two objects (the original one and the perturbed one) defined by the model is also small, and vice versa.

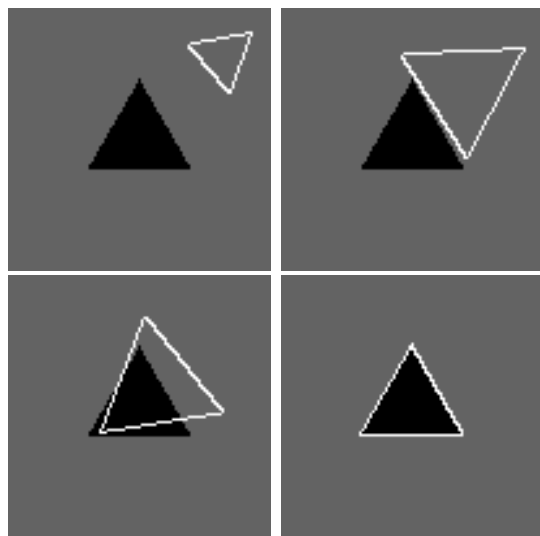


Figure 3.1 The shape comparison process between two equilateral triangles. In this example, $Index = 0$, and *the scale of perturbation* $r = 0$, which satisfies the inequalities in Theorem 2.

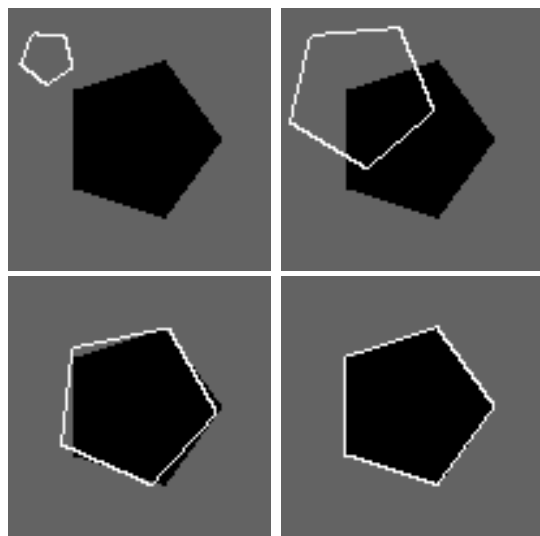


Figure 3.2 The shape comparison process between two equilateral pentagons. In this example, $Index = 0$, and *the scale of perturbation* $r = 0$, which satisfies the inequalities in Theorem 2.

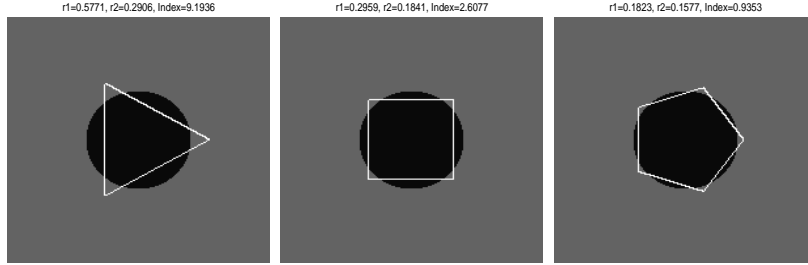


Figure 3.3 The comparison results between a disk and three equilateral polygons, that is, equilateral triangle, square and pentagon. For the left graph, the comparison between the circle and equilateral triangle yields $Index = 9.1936$ and $r = \max(r_1, r_2) = 0.5771$; For the middle graph, $Index = 2.6077$, $r = 0.2959$; For the right graph, $Index = 0.9353$, $r = 0.1823$. The values of $Index$ and the scale of perturbation r both decrease as the number of gons increase, which coincide with human visual.

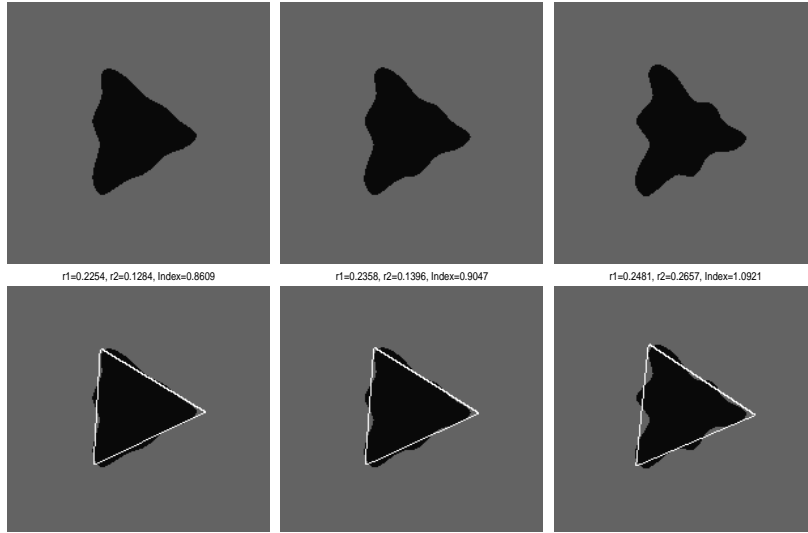


Figure 3.4 In this group of graphs, the top row shows three similar shapes, while the comparisons with equilateral triangles are listed accordingly, that is, the black objects in the same column are identical. For the left graph, the comparison yields $Index = 0.8609$ and $r = \max(r_1, r_2) = 0.2254$; For the middle graph, $Index = 0.9047$, $r = 0.2358$; For the right graph, $Index = 1.0921$, $r = 0.2657$. The three objects on the top row are similar, only differs from the magnitude of “oscillation”. From the listed values, it can be seen that as the “oscillation” increase, the values of $Index$ and the scale of perturbation r will become large. We provide a table (Table 1) to show the relation between $Index$ and the scale of perturbation r .

	$r = \max(r_1, r_2)$	<i>Index</i>	$Index/r^2$	$Index/r^4$
The left graph	0.2254	0.8609	16.9451	333.53
The middle graph	0.2358	0.9047	16.2711	292.63
The right graph	0.2657	1.0921	15.4696	219.12

Table 1 In this table, the left graph means the one in Figure 3.4, etc. From this table, we see as *the scale of perturbation* r increases, the value *Index* will increase, and *Index* is almost proportional to r^2 .

References:

- [1] T. Chan and L.A. Vese, Active contours without edges. *IEEE Transaction on Image Processing*, 10(2): 266-277, February 2001.
- [2] S. Osher and J. A. Sethian, Fronts Propagating with Curvature-Dependent Speed - Algorithms Based on Hamilton-Jacobi Formulations, *J. Comput. Phys*, Vol 79, 12 – 49, 1988.
- [3] N. Paragios, M. Rousson and V. Ramesh, Matching Distance Functions: A Shape-to-Area Variational Approach for Global-to-Local Registration. Copenhagen, Denmark, 2002.
- [4] M.Rousson and N. Paragios, Shape Priors for Level Set Representations.
- [5] H.K. Zhao, T. Chan, B. Merriman and S. Osher, A variational level set approach to multiphase motion. *J.Comput.Phys.*, 127 : 179 – 195, 1996.